Conf-9108108--3
BNL--46638
DE92 001778

Static and Dynamic Spin Fluctuations in the Spin Glass Doping Regime in $La_{2-x}Sr_xCuO_{4+y}$

by

R. J. Birgeneau,[a] N. Belk,[a] Y. Endoh,[b] R. W. Erwin,[c] M. A. Kastner,[a] B. Keimer,[a] and G. Shirane[d]

[a] Department of Physics, Massachusetts Institute of Technology, Cambridge, MA, 02139 USA

[b] Department of Physics, Tohoku University, Sendai 980, Japan

[c] National Institute of Standards and Technology, Gaithersburg, MD, 20899 USA

[d] Brookhaven National Laboratory, Upton, NY, 11973 USA

OCT 22 1991

Abstract

We review the results of neutron scattering studies of the static and dynamic spin fluctuations crystals of $La_{2-x}Sr_xCuO_{4+\delta}$ in the doping regime intermediate between the Néel and superconducting regions. In this regime the in-plane resistance is linear in temperature down to ~ 80 K with a crossover due to logarithmic conductance effects at lower temperatures. The static spin correlations are well-described by a simple model in which the inverse correlation length $\kappa(x,T) = \kappa(x,0) + \kappa(0,T)$. The most dramatic new result is the discovery by Keimer *et al.* that the dynamic spin fluctuations exhibit a temperature dependence which is a simple function of ω/T for temperatures $10\ K \leq T \leq 500\ K$ for a wide range of energies. This scaling leads to a natural explanation of a variety of normal state properties of the copper oxides.

To appear in the proceedings of ICNS'91 (Oxford England), Physica B (to be published)

MASTER

DISTRIBUTION OF THIS DOCUMENT IS UNLIMITED

I. Introduction

In virtually all cases, highly correlated electronic systems exhibit unusual and, most often, dramatic magnetic properties. This is true for mixed valent materials, heavy fermion systems and many organic conductors, in particular, those with competing spin density wave states. Without ambiguity, the most remarkable highly correlated electronic systems are the lamellar copper oxides.[1] As a function of doping, these materials evolve from antiferromagnetic Mott insulators to two-dimensional weakly localized spin glasses to novel metals exhibiting superconductivity at extraordinarily high temperatures.[2] Because of its unique properties as a probe of microscopic static and dynamic spin fluctuations, neutron scattering is playing an essential role in elucidating the fundamental properties of the copper oxide materials. However, the physics of the copper oxides is sufficiently complicated that neutron scattering alone has not been able to solve this problem. Rather, information from neutron experiments must be combined with data from other spectroscopic probes as well as data from transport, thermodynamic and magnetic measurements to produce a complete empirical picture.

In general, the neutron experiments themselves are very difficult so our characterization of the spin fluctuations in the lamellar copper oxides is still quite incomplete. So far, reliable experimental data are available only in the $La_{2-x}Sr_xCuO_4$ and $YBa_2Cu_3O_{6+\delta}$ systems. At this conference, J. Rossat-Mignod and collaborators[3] will discuss their work in the latter materials. In this review, therefore, we will largely confine our discussion to measurements in the $La_{2-x}Sr_xCuO_4$ materials. Our approach to this problem is that the antiferromagnetic Mott insulating, weakly localized spin glass and superconducting regimes each represent quite interesting and challenging basic physics problems in their own right. Further, to understand the high temperature superconductivity one will almost certainly have to understand the manner in which the properties of the CuO_2 sheets evolve between these three states. In this brief review we will not attempt to describe in detail all of the results in the $La_{2-x}Sr_xCuO_4$ system. Instead, we will focus on

the behavior in the intermediate spin glass regime where Keimer *et al.*[4] have recently obtained particularly interesting results.

II. Transport Measurements

Samples of $La_{2-x}Sr_xCuO_{4+\delta}$ which order magnetically typically exhibit the transport behavior of lightly doped semiconductors.[5] The in-plane room temperature resistivity decreases rapidly with increasing x or δ and there is substantial evidence for an insulator to metal transition <u>within</u> the CuO_2 sheets at a hole concentration of about 1.5%.[6] This is suggestively close to the hole concentration at which the Néel order vanishes although a direct causal relationship between these two phenomena has not yet been established.

In the spin glass regime, the between-plane conductivity is semiconducting for all temperatures below 500 K. On the other hand, the in-plane behavior is quite striking. We show in Fig. 1 results of measurements of the in-plane resistivity of a small single crystal of $La_{1.96}Sr_{0.04}CuO_4$. This crystal was cut from th sample used in the neutron experiments of Keimer *et al.*[4] to be discussed later in this review. The transport data obtained in this sample are typical of those found in high quality single crystals of $La_{2-x}Sr_xCuO_{4+\delta}$ for $0.02 \leq x \leq 0.06$.[7] At temperatures above ~ 80 K the resistivity varies linearly with temperature. The slope, normalized to the inverse of the carrier concentration, is comparable to that found in single crystals of $YBa_2Cu_3O_7$.

As seen in the lower panel of Fig. 1, at low T the conductance is proportional to $\log_{10}T$ over more than a decade of temperature. The proportionality to $\log_{10}T$ is typical of conventional 2D disordered metals,[8] but in those the log term is usually a small correction to the total conductance, whereas it dominates the conductance in $La_{1.96}Sr_{0.04}CuO_{4+y}$ for T < 80 K. From a different viewpoint, however, the $\log_{10}T$ term does not seem exceptionally large, since, as predicted by the theories of weak localization and

interaction,[8] we find that the coefficient of the lnT conductance is ~ e^2/h whenever the conductance is $\gtrsim e^2/h$.

The magnetoresistance of these crystals is very different from that of conventional 2D disordered metals. Specifically, one finds that the magnetoresistance is isotropic in the field direction and that to a good approximation it scales linearly with H/T for H/T > 0.1.[7] This unusual behavior almost certainly results from the strong coupling between the spin of the charge carriers and the fluctuating Cu^{2+} spins.

III. Instantaneous Spin Correlations

In this section we review some very recent results by Keimer *et al.*[4] on the instantaneous spin correlations in $La_{2-x}Sr_xCuO_4$. We remind the reader that the instantaneous spin correlation function $S(\vec{Q}) = \frac{1}{2\pi}\sum_{\vec{r}} e^{i\vec{Q}\cdot\vec{r}} \langle \vec{S}_{\vec{0}} \cdot \vec{S}_{\vec{r}} \rangle$ is obtained by integrating the Van Hove scattering function $S(\vec{Q},\omega)$ over ω at fixed $\vec{Q}$. This is, in general, a difficult process experimentally. In one-layer materials such as $La_{2-x}Sr_xCuO_4$ one may utilize the trick original. discovered by Birgeneau *et al.*;[9] one arranges the two-axis spectrometer scattering geometry such that the outgoing neutron is perpendicular to the CuO_2 sheets. In that case one effectively integrates from ~ – kT to E_i in energy and one obtains a good approximation to $S(\vec{Q})$ provided that the dominant fluctuations have energies less than E_i. This will be the case for all measurements reviewed here. Unfortunately, because of the strong correlations between the spins in adjacent layers in $YBa_2Cu_3O_{6+\delta}$ this trick cannot be employed in that system; consequently there are no reliable measurements of the correlation lengths in the 123 system. However, educated guesses can be made from Q-scans at fixed energies.

We show in Fig. 2 results from an extensive set of measurements reported in Ref. [4]. This figure shows inverse correlation lengths κ obtained from fits of the measured $S(\vec{Q})$ to a Lorentzian $A/(\kappa^2 + q_{2D}^2)$; here $\vec{q}_{2D} = \vec{Q}_{2D} - \vec{G}_{(100)}$ where $\vec{G}_{(100)}$ is the antiferromagnetic superlattice position and $\vec{Q}_{2D}$ is the in-plane projection of the momentum

transfer. The pure $La_2CuO_{4.0}$ sample orders at T_N = 325 K. For an ideal 2D antiferromagnetic Heisenberg model the correlation length is predicted to have the form

$$\xi = \frac{e}{8}\,\frac{\hbar c}{2\pi\rho_s}\,\exp\left[\frac{2\pi\rho_s}{T}\right]\left[1 - 0.5\,\frac{T}{2\pi\rho_s}\right] + 0\left((T/2\pi\rho_s)^2\right) \qquad (1)$$

where $\hbar c$ is the spin wave velocity and ρ_s is the spin stiffness.[10],[11] The solid line in Fig. 2 for the $La_2CuO_{4.0}$ data is Eq. (1) with $2\pi\rho_s$ = 150 meV ≃ 1.1 J_{nn} where J_{nn} is the nearest-neighbor exchange. Simple spin wave theory predicts $2\pi\rho_s = 0.94\ J_{nn}$.[10]

Clearly Eq. (1) works well but not perfectly; specifically there seems to be a systematic pattern in the disagreement between experiment and the 2D Heisenberg model theory. In La_2CuO_4 there are, in addition to the Heisenberg coupling term, small but important XY anisotropy and antisymmetric exchange terms in the spin Hamiltonian.[12] Qualitatively, these terms seem capable of accounting for the discrepancies; however, a quantitative theory is lacking.

The correlation length data in the doped samples are quite striking. It is evide from Fig. 2 that the inverse correlation length at low temperatures increases rapidly with increasing Sr^{2+} concentration. It should be noted that for the Sr-doped crystals the authors of Ref. [4] used their samples "as-grown." Thus the hole concentration will in general be somewhat different from the Sr concentration, albeit in a systematic fashion. At high doping levels the low temperature correlation length is of order the average separation between the holes. Quantitative interpretation of the data in Fig. 2 shows that this relationship breaks down near x ≃ 0.02 as it must since for smaller hole concentrations long range order is achieved, that is $\kappa \rightarrow 0$.

Keimer *et al.*[4] have discovered that in the spin-glass crossover regime the inverse correlation length for all temperatures between 10 K and 500 K, is simply given by

$$\kappa(x,T) = \kappa(x,0) + \kappa(0,T) \qquad (2)$$

The solid lines in Fig. 2 correspond to Eq. (2) with $\kappa(x,0)$ fixed by the low temperature data and $\kappa(0,T)$ determined from Eq. (1). This behavior is very different from what one would expect from the non-linear sigma model in the quantum disordered regime.[10] There is currently no theoretical model for the doped copper oxides which predicts this simple, elegant behavior. Clearly extension of experiments of this precision into the superconducting concentration regime is very important.

IV. Dynamic Spin Fluctuations

Keimer *et al.*[4] have studied in detail the low energy spin dynamics in the sample $La_{1.96}Sr_{0.04}CuO_4$. Complementary experiments by Hayden *et al.*[13] have been carried out in $La_{1.95}Ba_{0.05}CuO_4$. These two studies are generally consistent with each other. We shall emphasize the former experiments since they lead to a scaling function for $\int d^2q\, \chi''(q,\omega)$ which has broad significance for our understanding of transport, magnetic and spectroscopic properties of the doped copper oxides.

It is shown in Ref. [4] that in $La_{1.96}Sr_{0.04}CuO_4$ the fluctuations are centered around the (π,π) position (square lattice notation) and that there is no measurable scattering at other high symmetry positions such as $(\pi,0)$ and $(2\pi,0)$. The latter result excludes a number of theoretical models. The peaks are commensurate to within the accuracy of the experiment. Figure 3 shows resolution corrected integrated intensities of the scattering around (π,π) as a function of temperature. The solid lines are the predictions of a theoretical model which we shall discuss shortly. One of the most notable features of the data is that for each energy the intensity peaks at a temperature of $T \simeq 2\omega$. This led Keimer *et al.*[4] to plot the data in a scaled form in terms of ω/T.

Figure 4 shows $\chi''(\vec{Q},\omega)$ integrated around the (π,π) position. The data are normalized at the maximum intensity in Fig. 3 and the overall scale is chosen such that the integrated susceptibility for $\omega/T > 1$ is ~ 1. We shall discuss the significance of this normalization below. The results shown in Fig. 4 are clearly quite striking. All of the data

for temperatures between 10 K and 500 K and energies between 4.5 meV and 12 meV fall on a single universal curve when plotted in this fashion. This scaling occurs in spite of the fact that the correlation length is nearly independent of temperature over the entire temperature interval. We also note that there is no difference for data at temperatures above and below 100 K. Thus $Im\chi(\vec{Q},\omega)$, along with the static correlations, is insensitive to localization effects as one might have expected on physical grounds since such localization typically involves the behavior of the carrier wave functions at large distances.

In order to obtain a parametrization of their data, Keimer *et al.*[4] use the simplest model consistent with relaxational dynamics in a disordered antiferromagnet:

$$\chi(\vec{q},\omega) = \frac{\xi^2}{1 + q^2\xi^2 - i\, f(\frac{\omega}{\Gamma})} \tag{4}$$

This formula has also been used by other research groups and is therefore useful for comparison with their results. In mean field theory, $\Gamma \sim \xi^{-2}$. The data of Fig. 3 suggest instead that one writes *ad hoc* $\Gamma \sim T$, although $\xi \sim$ const. Time reversal symmetry then requires that the function $f(\omega/T)$ can generally be written as $f(\omega/T) = \sum_{n=1,3\ldots} a_n(\omega/T)^n$. One then obtains

$$\int_{(\pi,\pi)} d^2q\, Im\chi(\vec{q},\omega) = I(\omega) \arctan\left(a_1(\tfrac{\omega}{T}) + a_3(\tfrac{\omega}{T})^3 + \ldots\right) \tag{5}$$

where the factor $I(\omega)$ gives the ω-dependence of the integrated spin susceptibility at $T = 0$. The solid line in Fig. 4 represents the best fit to this form, normalized to unity at large ω/T with $a_1 = 0.43$ and $a_3 = 10.5$. Inclusion of higher order terms does not improve the fit. The solid lines in Fig. 3 are also calculated from this formula. The zero temperature behavior $I(\omega)$ is given in the inset in Fig. 4. Clearly, the parametrization of Eq. (5) is very good, however, we should point out that, while Eq. (5) describes the integrated intensity very well, the lineshape of the measured peaks is in fact not described by Eq. (4). This

form would predict a divergence of the peak width at low temperatures, whereas the width of the observed peaks is temperature independent. As a matter of fact, the simplest functional form of $Im\chi(\vec{Q},\omega)$ consistent with all of the data is simply the product of the right hand side of Eq. (5) with the two-dimensional Lorentzian static structure factor determined in the energy-integrating experiments above.

The experiments of Ref. [4] cover a wide range of temperatures $10\ K \leq T \leq 500\ K$ but only a narrow range of energies. Hayden *et al.*[13] on the other hand have studied the dynamics in $La_{1.95}Ba_{0.05}CuO_4$ up to energies of order 90 meV. They find that $I(\omega)$ is nearly constant up to very high energies. Further they find that for $80\ K \leq T \leq 250\ K$ their data are well described by Eq. (5) with $I(\omega)$ fixed at a constant, $a_1 \simeq 2$ and $a_3 = 0$. They obtain an apparent breakdown of this scaling at lower temperatures. However, in their analysis $I(\omega)$ is fixed to be a constant independent of frequency and they omit the higher order terms in (ω/T); thus it is not clear how significant this discrepancy with Keimer *et al.*[4] is.

We note that Eq. (5) is consistent with the Marginal Fermi Liquid Model of Varma *et al.*[14] which hypothesizes, as part of a phenomenological picture of the fluctuations in the optimal superconducting concentration regime, $Im\chi \sim \omega/T$ for $|\omega| \ll T$ and ~ 1 for $|\omega| \gg T$. The physics, however, appears to be more general than that assumed in Ref. [14] since Eq. (5) works well for $La_{2-x}Sr_xCuO_{4+\delta}$ [15] and $YBa_2Cu_3O_{6+\delta}$ [16] samples with antiferromagnetic correlation lengths varying between 150 Å and 10 Å.

V. Implications of the Neutron Results for Other Properties

Many physical quantities depend directly on $Im\chi(\vec{Q},\omega)$. For example, Moriya and co-workers [17] have argued that the electrical resistivity due to antiferromagnetic fluctuations should scale like

$$R \sim T \int_{-\infty}^{\infty} \left(\frac{\omega}{T}\right) d\left(\frac{\omega}{T}\right) \frac{e^{\omega/T}}{(e^{\omega/T} - 1)^2} \int d\vec{Q}\, Im\chi(\vec{Q},\omega). \tag{6}$$

Clearly, any form for $\int d\vec{Q}\, Im\chi(\vec{Q},\omega)$ which is homogeneous in ω/T will lead to a resistance linear in T due to spin fluctuations. The data of Ref. [4] indeed manifest such homogeneity provided $I(\omega) \sim$ constant over the important range of ω. As shown in the insert in Fig. 4(a), $I(\omega)$ is indeed approximate'y constant, except for the point at 4.5 meV. Heuristically, for $\omega \geq v\kappa \sim 20$ meV in $La_{1.96}Sr_{0.04}CuO_4$ one expects a crossover to spin wave behavior, $I(\omega) \sim$ constant. This is confirmed by the results of Hayden *et al.*[13] This in turn implies $R \sim T$. Thus neutron scattering has provided a natural explanation for one of the most striking properties of the normal state of the copper oxides.

It is also apparent from Eq. (6) that one would expect an isotropic, negative magnetoresistance due to the diminution in $Im\chi$ by an applied field. This agrees with the recent results of Preyer *et al.*[17] However, a detailed theoretical treatment is required to explain their observed H/T scaling [7] although the measured ω/T scaling is certainly suggestive. The above arguments also seem capable of explaining the optical conductivity.[18] Finally, Eq. (5) appears to be consistent with Cu^{2+} NMR relaxation data in both $La_{2-x}Sr_xCuO_4$[19] and $YBa_2Cu_3O_{6+\delta}$.[20]

VI. Conclusions

It is clear that very significant progress has been made in our characterization of the magnetism in the intermediate doping regime in the copper oxides. Although we have not explicitly reviewed the relevant data here this scaling approach also works very well in $YBa_2Cu_3O_{6+\delta}$ samples in the intermediate doping regime.[16] As discussed by Shirane *et al.*[21] and by Rossat-Mignod *et al.*[3] the behavior in the fully superconducting regime is more elaborate. Specifically, gaps seem to appear at low energies and temperatures. This represents a significant modification of Eq. (5). Clearly much work remains to understand the evolution in the spin dynamics between the spin glass and superconducting doping

regimes. We thus expect that neutron scattering will continue to play a central role in elucidating the physics of high temperature superconductors for the indefinite future.

Acknowledgements

We would like to thank Elihu Abrahams, Gabriel Aeppli, Sudip Chakravarty, Vic Emery, Steve Kivelson, Jeff Lynn, Patrick Lee, Peter Littlewood, John Tranquada, and Chandra Varma for helpful discussions. The research at MIT was supported by the National Science Foundation under Grants No. DMR 90-22933, DMR 90-14839 and DMR 90-07825. Work at Brookhaven was carried out under contract DE-AC02-76CH00016, Division of Materials Science, US Department of Energy.

References

[1] For general reviews see "Physical Properties of High Temperature Superconductors," Ginsberg, D. M. (ed). Vol. I, II Singapore, World Scientific, 1990.

[2] A. Aharony, R. J. Birgeneau, A. Coniglio, M. A. Kastner and H. E. Stanley, Phys. Rev. Lett. **60**, 1330 (1988).

[3] J. Rossat-Mignod *et al.* (unpublished).

[4] B. Keimer, R. J. Birgeneau, A. Cassanho, Y. Endoh, R. W. Erwin, M. A. Kastner and G. Shirane (unpublished).

[5] N. W. Preyer, R. J. Birgeneau, C. Y. Chen, D. R. Gabbe, H. P. Jenssen, M. A. Kastner, P. J. Picone and T. Thio, Phys. Rev. B **39**, 11563 (1989).

[6] C. Y. Chen, N. W. Preyer, P. J. Picone, M. A. Kastner, H. P. Jenssen, D. R. Gabbe, A. Cassanho and R. J. Birgeneau, Phys. Rev. Lett. **63**, 2307 (1989).

[7] N. W. Preyer. M. A. Kastner, C. Y. Chen, R. J. Birgeneau and Y. Hidaka, Phys. Rev. B **44**, 4[illegible] (1991).

[8] For a review see P. A. Lee and T. V. Ramakrishnan, Rev. Mod. Phys. **57**, 287 (1985).

[9] R. J. Birgeneau, J. Skalyo Jr. and G. Shirane, Phys. Rev. **33**, 1736 (1971).

[10] S. Chakravarty, B. I. Halperin and D. R. Nelson, Phys. B **39**, 2344 (1989).

[11] P. Hasenfratz and F. Niedermeyer (unpublished).

[12] C. J. Peters, R. J. Birgeneau, M. A. Kastner, H. Yoshizawa, Y. Endoh, J. Tranquada, G. Shirane, Y. Hidaka, M. Oda, M. Suzuki and T. Murakami, Phys. Rev. B **37**, 9761 (1988).

[13] S. M. Hayden, G. Aeppli, H. Mook, D. Rytz, M. F. Hundley and Z. Fisk, Phys. Rev. Lett. **66**, 821 (1991).

[14] C. M. Varma, P. B. Littlewood, S. Schmitt-Rink, E. Abrahams and A. E. Ruckenstein, Phys. Rev. Lett. **63**, 1996 (1989).

[15] Y. Endoh *et al.* (unpublished).

[16] R. J. Birgeneau (unpublished).

[17] T. Moriya, Y. Takahashi and K. Ueda, J. Phys. Soc. Jpn. **59**, 2905 (1990).

[18] T. Moriya and Y. Takahashi, J. Phys. Soc. Jpn. **60**, 776 (1991).

[19] T. Imai, K. Yoshimura, T. Uemura, H. Yasuoka and K. Kosuge, J. Phys. Soc. Jpn. **59**, 3846 (1990).

[20] See for example C. H. Pennington and C. P. Slichter in Ref. 1, II. p. 269.

[21] G. Shirane, R. J. Birgeneau, Y. Endoh, P. Gehring, M. A. Kastner, K. Kitazawa, H. Kojima, I. Tanaka, T. R. Thurston and K. Yamada, Phys. Rev. Lett. **63**, 330 (1989).

Figure Captions

Fig. 1 (a) In-plane resistivity ρ_a vs T in $La_{1.96}Sr_{0.04}CuO_4$. (b) Same data plotted as conductance.

Fig. 2 Inverse magnetic correlation length of pure (T_N = 325 K) and Sr-doped crystals of La_2CuO_4. The solid line through the undoped crystal data is the prediction of Chakravarty, Halperin and Nelson[10] and Hasenfratz and Niedermeyer[11] for the spin-1/2 Heisenberg antiferromagnet while for the doped systems the solid lines are $\kappa(x,T) = \kappa(x,0) + \kappa(0,T)$.

Fig. 3 Intrinsic 2D integrated intensities of the scattering profiles at various temperatures and energy transfers. The solid lines are the form $(1 - e^{-\omega/T})^{-1} \tan^{-1} (a_1(\omega/T) + a_3(\omega/T)^3)$ with $a_1 = 0.43$, $a_3 = 10.5$. The dashed line associated with the 4.5 meV data is the simplest marginal Fermi liquid (Ref. [14]) prediction with $a_1 = 2.2$ and $a_2 = 0$.

Fig. 4 Normalized integrated spin susceptibility around (π,π) as a function of the scaling variable ω/T. The insert in panel (a) shows the normalization constant. Panel (b) is a closeup of panel (a). The lines are the function $2/\pi \tan^{-1} (a_1(\omega/T) + a_3(\omega/T)^3)$ with $a_1 = 0.43$, $a_3 = 10.5$ (solid line) and $a_1 = 2.2$, $a_3 = 0$ dashed line.

DISCLAIMER

This report was prepared as an account of work sponsored by an agency of the United States Government. Neither the United States Government nor any agency thereof, nor any of their employees, makes any warranty, express or implied, or assumes any legal liability or responsibility for the accuracy, completeness, or usefulness of any information, apparatus, product, or process disclosed, or represents that its use would not infringe privately owned rights. Reference herein to any specific commercial product, process, or service by trade name, trademark, manufacturer, or otherwise does not necessarily constitute or imply its endorsement, recommendation, or favoring by the United States Government or any agency thereof. The views and opinions of authors expressed herein do not necessarily state or reflect those of the United States Government or any agency thereof.

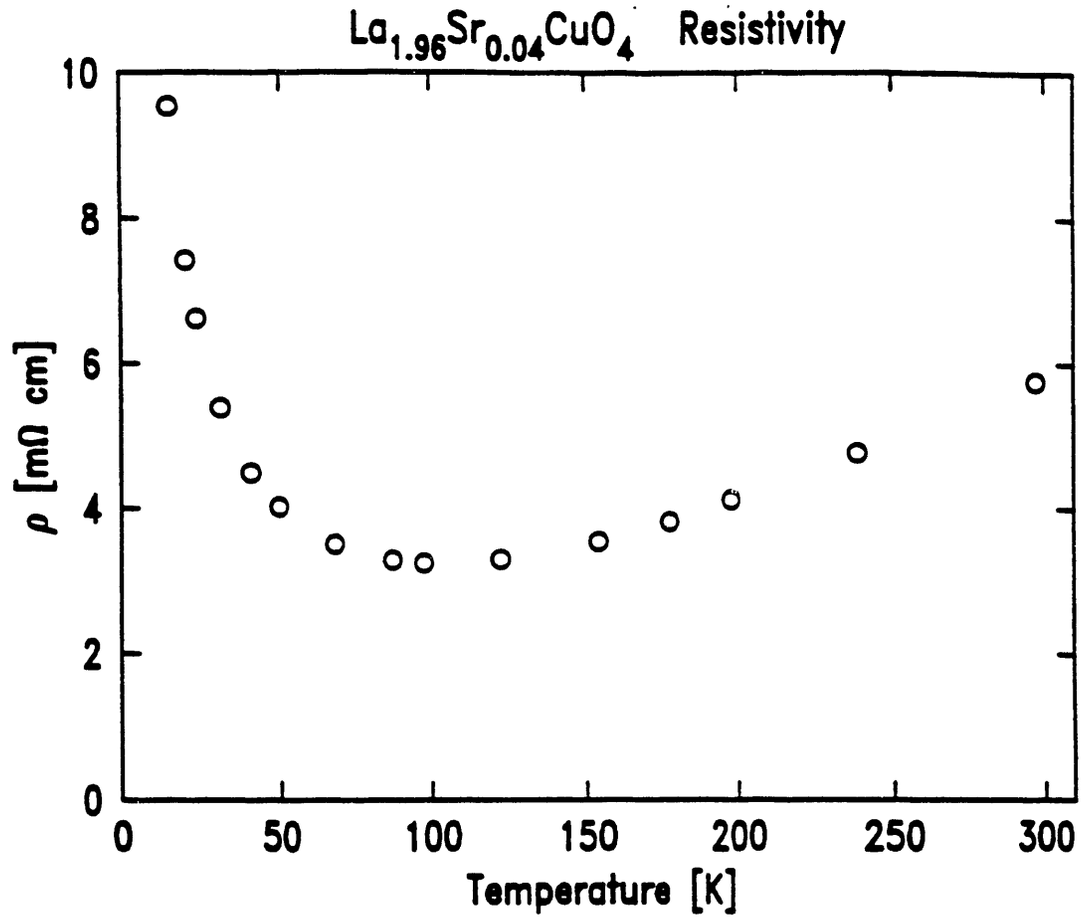
La1.96Sr0.04CuO4 Resistivity
ρ [mΩ cm]
Temperature [K]
0
2
4
6
8
10
0
50
100
150
200
250
300

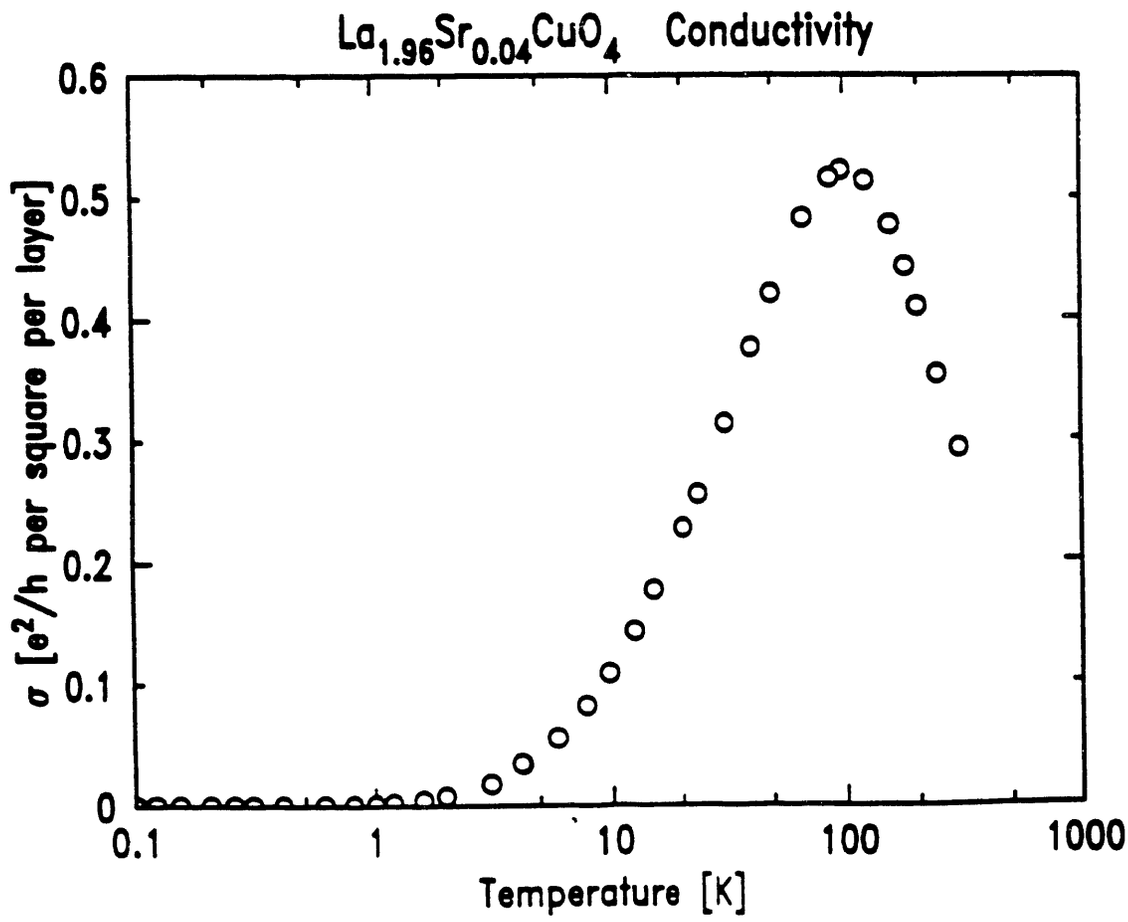
La1.96Sr0.04CuO4 Conductivity
σ [e²/h per square per layer]
Temperature [K]
0
0.1
0.2
0.3
0.4
0.5
0.6
0.1
1
10
100
1000

Fig. 1

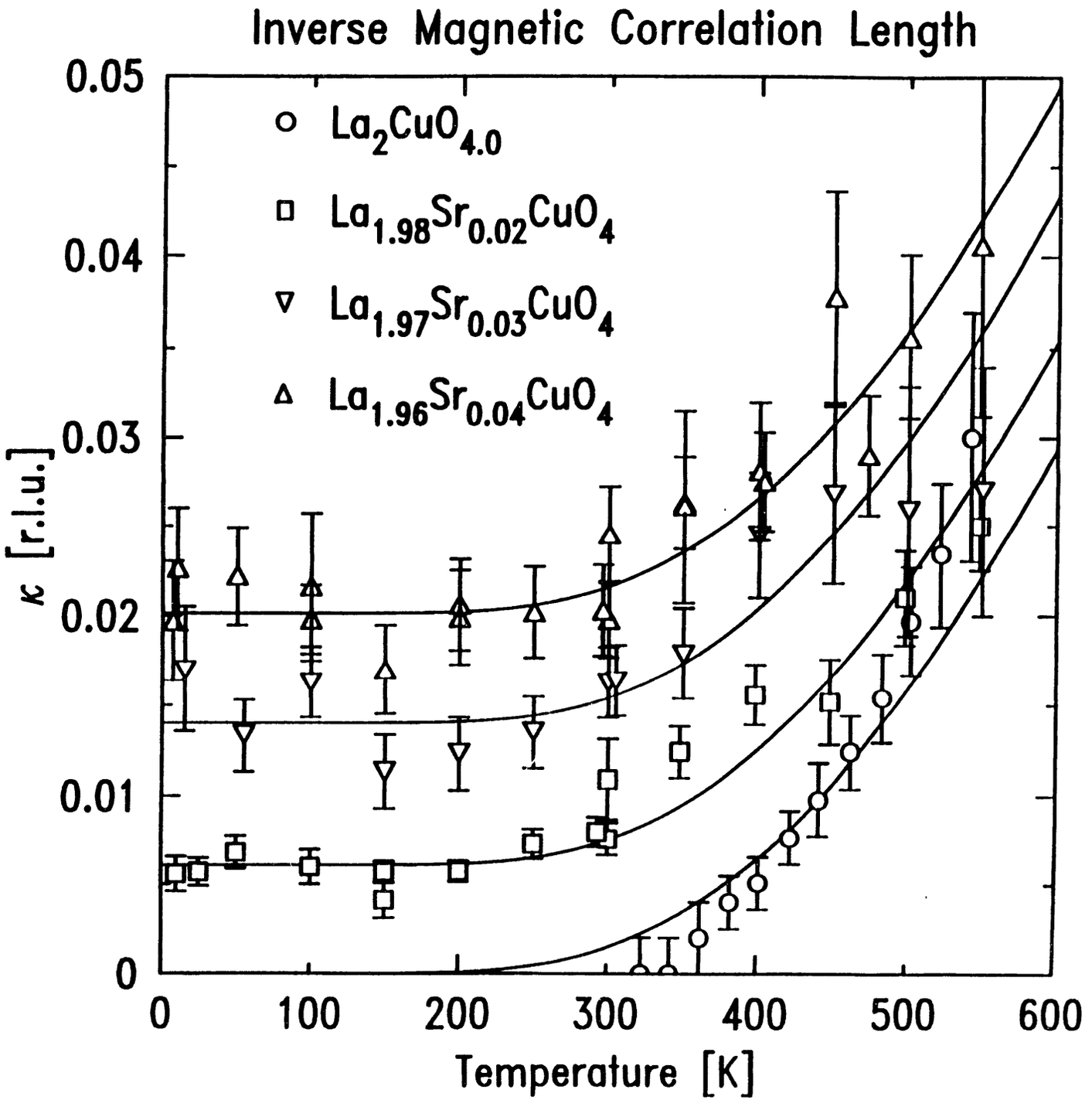
Inverse Magnetic Correlation Length
$La_2CuO_{4.0}$
$La_{1.98}Sr_{0.02}CuO_4$
$La_{1.97}Sr_{0.03}CuO_4$
$La_{1.96}Sr_{0.04}CuO_4$
κ [r.l.u.]
0.05
0.04
0.03
0.02
0.01
0
0
100
200
300
400
500
600
Temperature [K]

Fig. 2

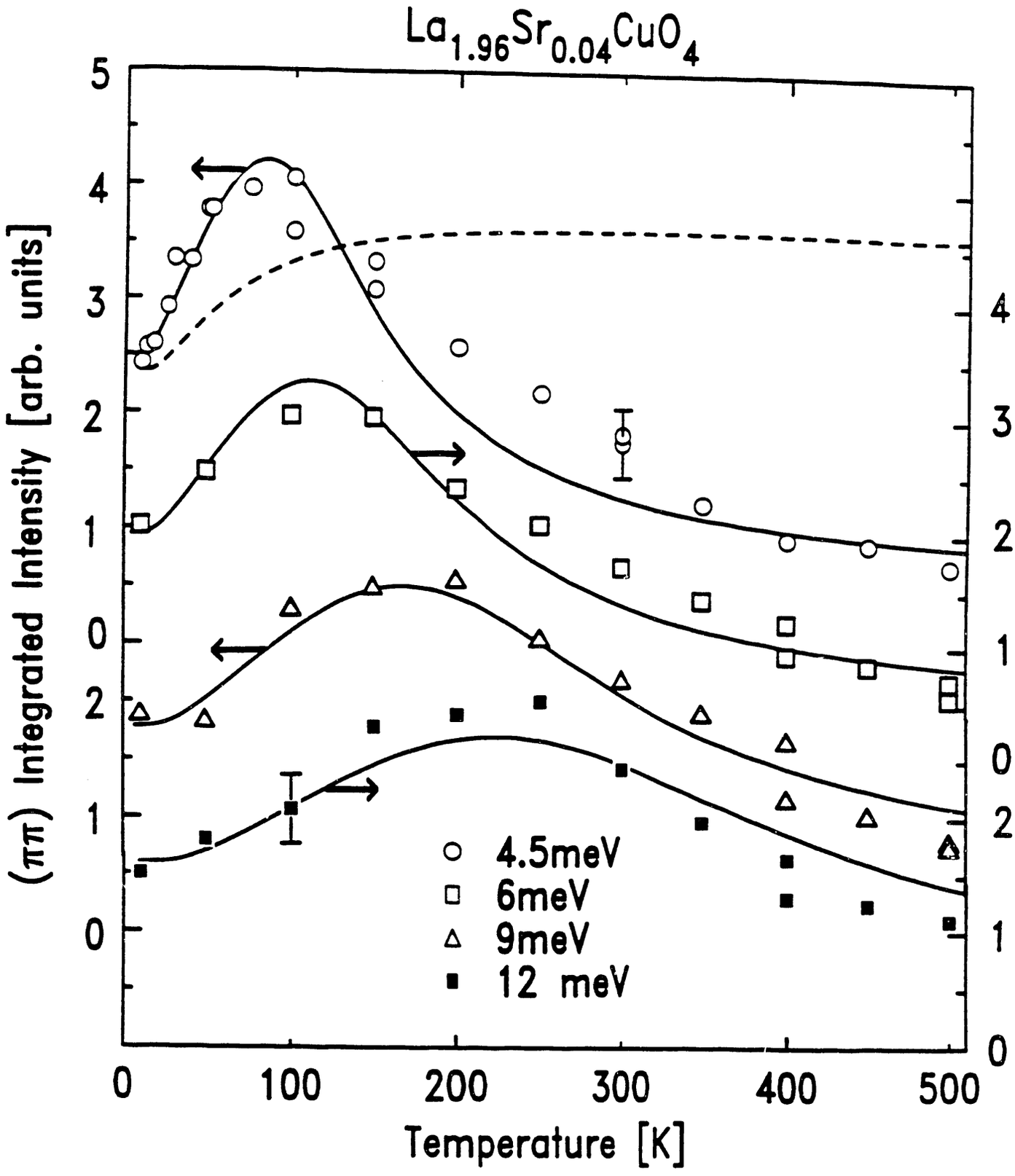
La1.96Sr0.04CuO4
(ππ) Integrated Intensity [arb. units]
Temperature [K]
4.5meV
6meV
9meV
12 meV
0
100
200
300
400
500
0
1
2
3
4
5

Fig. 3

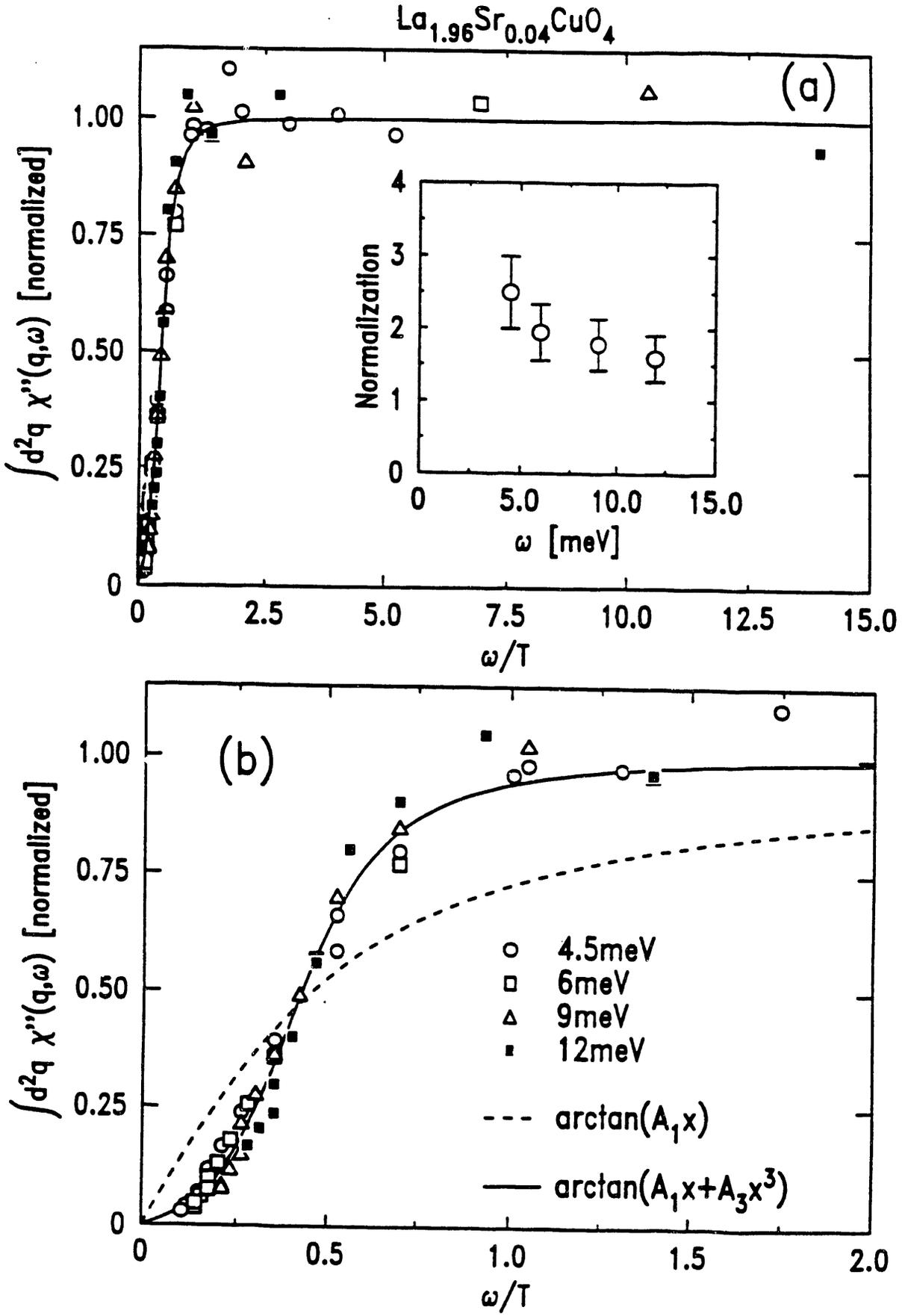
La1.96Sr0.04CuO4
(a)
(b)
∫d²q χ''(q,ω) [normalized]
ω/T
Normalization
ω [meV]
4.5meV
6meV
9meV
12meV
arctan(A1x)
arctan(A1x+A3x³)

Fig. 4

END

DATE FILMED

11/19/91